Received: 23 June 2022 | Revised: 6 September 2022 | Accepted: 6 September 2022

DOI: 10.1111/jace.18821

Journal of the American Ceramic Society

RAPID COMMUNICATION

Resistive-switching in yttria-stabilized hafnia ceramics

Meshari Alotaibi[1,2] | **Fawaz Almutairi**[1,3] | **Anthony R West**[1]

[1]Department of Materials Science and Engineering, University of Sheffield, Sheffield, UK

[2]Department of Chemistry, Faculty of Science, Taif University, Taif, Saudi Arabia

[3]Department of Physics, College of Science, Al Imam Mohammad Ibn Saud Islamic University (IMISU), Riyadh, Saudi Arabia

Correspondence
Anthony R West, Department of Materials Science & Engineering, University of Sheffield, Mappin St, Sheffield S1 3JD, UK.
Email: a.r.west@sheffield.ac.uk

Abstract

Yttria-stabilized hafnia ceramics are high-temperature oxide ion conductors that lose a small amount of oxygen, both at high temperatures and on the application of a small dc bias. At zero applied bias, a small amount of *p*-type conductivity is present. This increases with low bias and is attributed to reactions initiated at the positive electrode/ceramic interface. With a further increase in bias, *n*-type conductivity is initiated at the negative electrode/ceramic interface. After a short time-lapse, the overall conductivity increases rapidly by 1.5–3 orders of magnitude and is reversible, with hysteresis, on subsequent removal of the bias. Switching has been observed over the range 457–531°C and is sensitive to both temperature and oxygen partial pressure in the surrounding atmosphere. This is the first example of low field, resistive switching in bulk hafnia ceramics, in contrast to most examples of resistive switching which are observed in nanometre-thick devices using similarly applied voltages.

KEYWORDS
dc voltage, impedance spectroscopy, resistive switching, yttria-stabilized hafnia

1 | INTRODUCTION

There is much current interest in resistive switching (RS) phenomena in thin film devices for memristive applications.[1–6] An essential feature of these devices appears to be the creation of nano-dimensional conducting filaments on the application of a small voltage during a pre-forming stage. These filaments break and reform during subsequent switching.[1–6] Resistive switchings may also occur by other mechanisms, including the well-known temperature-induced, metal-insulator Verwey transition in magnetite and VO_2 that is associated with structural changes at a crystallographic phase transition.[7–9]

The recently-discovered phenomenon of flash sintering (FS)[10–13] is based on the application, at high temperatures, of a moderate voltage, typically 50–100 V, across powder compacts, ceramics, or single crystals. The onset of FS is accompanied by rapid increases in conductivity. Recent studies of flash sintering of gadolinium doped ceria,[14] showed that under the application of an electric field and heat, the flash event was linked with *n*-type conduction which was initiated at the negative electrode and extended with increasing time to the positive electrode.

Thin films of pure and doped HfO_2 have received much attention recently because of their ferroelectric and resistive-switching behavior.[15,16] RS has also been demonstrated in several other binary metal oxides including NiO, TiO_2, ZrO_2, Al_2O_3, and Nb_2O_5, or ternary metal oxides such as Cr-doped $SrTiO_3$ and $Na_{0.5}Bi_{0.5}TiO_3$.[6,17,18] A common characteristic is that RS occurs in nanometer-thick films and devices. The mechanism of RS is often attributed to the electromigration of either oxygen vacancies or metal cations such as Cu or Ag. These

mobile species can join up to form a conductive pathway between opposite electrodes and the forming/breaking of these conducting pathways leads to resistive switching.[9,19,20]

In bulk ceramics, a different type of switching of Ca-doped $BiFeO_3$ at modest temperatures was induced by the application of a small dc voltage. It was not associated with a crystallographic transition and the resulting high conductivity ON state was isotropic, which excluded the possibility of a switching mechanism based on the making and breaking of conducting filaments.[21] Here we report resistive switching at high temperatures in bulk ceramics of oxide ion conducting, yttria-stabilized hafnia (YSH); it is the second example of RS in bulk ceramics. This is not associated with a phase transition and occurs in materials that are electronically insulating when prepared by standard synthesis and processing procedures in the air. An essential pre-forming step appears to be the field-induced generation of bulk electronic conductivity at opposite electrodes associated with two carriers, holes and electrons; oxygen exchange with the surrounding atmosphere is also important and, in combination with the application of a bias, leads to the creation of a p-i-n junction whose forming and breaking is responsible for subsequent resistive switching.

2 | EXPERIMENTAL PROCEDURE

Ceramic samples of composition $Hf_{1-x}Y_xO_{2-x/2}$: x = 0.15, YSH15, were prepared, as described previously[22] by solid-state synthesis using HfO_2 and Y_2O_3. These were reacted in air in alumina crucibles at 1300°C for 10 h, pressed into pellets, and sintered at 1750°C for 16 h with heating and cooling rates of 5°C/min to give pellets ~0.9 mm thick, ~8.3 mm diameter with densities of ~92% and grain size~ 30–50 μm.[22] The densities were measured by two ways 1) using Archimedes' principle in which a pellet was weighed, both in air and on subsequent immersion in water and 2), by calculating the density of a pellet from its volume and mass and dividing by the expected density calculated from the unit cell volume and mass of the cell contents. Both ways gave similar values of relative density.

For impedance spectroscopy (IS) measurements, gold electrodes were pasted on opposite faces of sintered pellets, dried at 850°C for 2 h and the pellets were loaded into a conductivity jig, and placed inside a tube furnace. IS measurements were made using either a Modulelab XM Solartron analyzer over the range 0.01 Hz–1 MHz or an Agilent 4249A Precision Impedance Analyser, frequency range 40 Hz-1 MHz for IS measurements at the same time as a *dc* voltage was applied. On application of a dc bias, 2 min were allowed before IS measurements; in some cases, IS measurements were repeated at 2 min intervals. Impedance data corrected for overall sample geometry and blank permittivity of the jigs are reported in resistivity and permittivity units of Ωcm and F/cm.

3 | RESULTS AND DISCUSSION

Typical IS data are shown in Figure 1; three temperatures are chosen that show, collectively, the full range of impedance response. Three main components are apparent in the impedance complex plane plots (A–C) and assigned, with decreasing frequency, to bulk, grain boundary, and sample-electrode impedances. This is confirmed by capacitance, C' plots (D) obtained using the same data sets which show a limiting high-frequency capacitance plateau, an intermediate frequency inflection, and a limiting low-frequency plateau of approximate values 2 pF, 100 pF, and 300 μF, respectively. The high value of the sample-electrode capacitance indicates that the samples are primarily oxide ion conductors.[22]

The total conductivity of YSH15 as a function of voltage at two temperatures, 457 and 501°C, and in three different atmospheres, O_2, air, and N_2 is shown in Figure 2. Although these are total conductivities, the impedance complex plane plots, Figure 1, show that at lower temperatures, the total conductivity is dominated by the bulk conductivity, and therefore the changes seen in Figure 2 also approximate bulk conductivity changes. The total conductivity–voltage profile, Figure 2, has the same general appearance in all six datasets. The conductivity is voltage-independent initially but then increases rapidly, associated with the onset of electronic conduction, before undergoing a sharp increase by 1.5 to 2.5 orders of magnitude to reach a steady ON state after which no further conductivity increase occurs. At each temperature, the magnitude of the conductivity increased and the steady state value was greatest in N_2 and least in O_2; also the voltage at which switching occurred is lowest in N_2 and highest in O_2. On decreasing the applied voltage, the high conductivity state is retained to lower applied voltages, leading to hysteresis loops followed by a sudden return to the original conductivity, the OFF state.

In all six cases, transition to the ON state is accompanied by a temperature rise of about 8°C which is reversed on return to the OFF state; the temperature increase, is measured by a thermocouple in close proximity (~2 mm) to the sample, is attributed to Joule heating caused by reduction in sample resistance without change in the applied voltage. The initial conclusion from these results is, therefore, that the bulk impedance of YSH15 undergoes a reversible, resistive switching transition at high

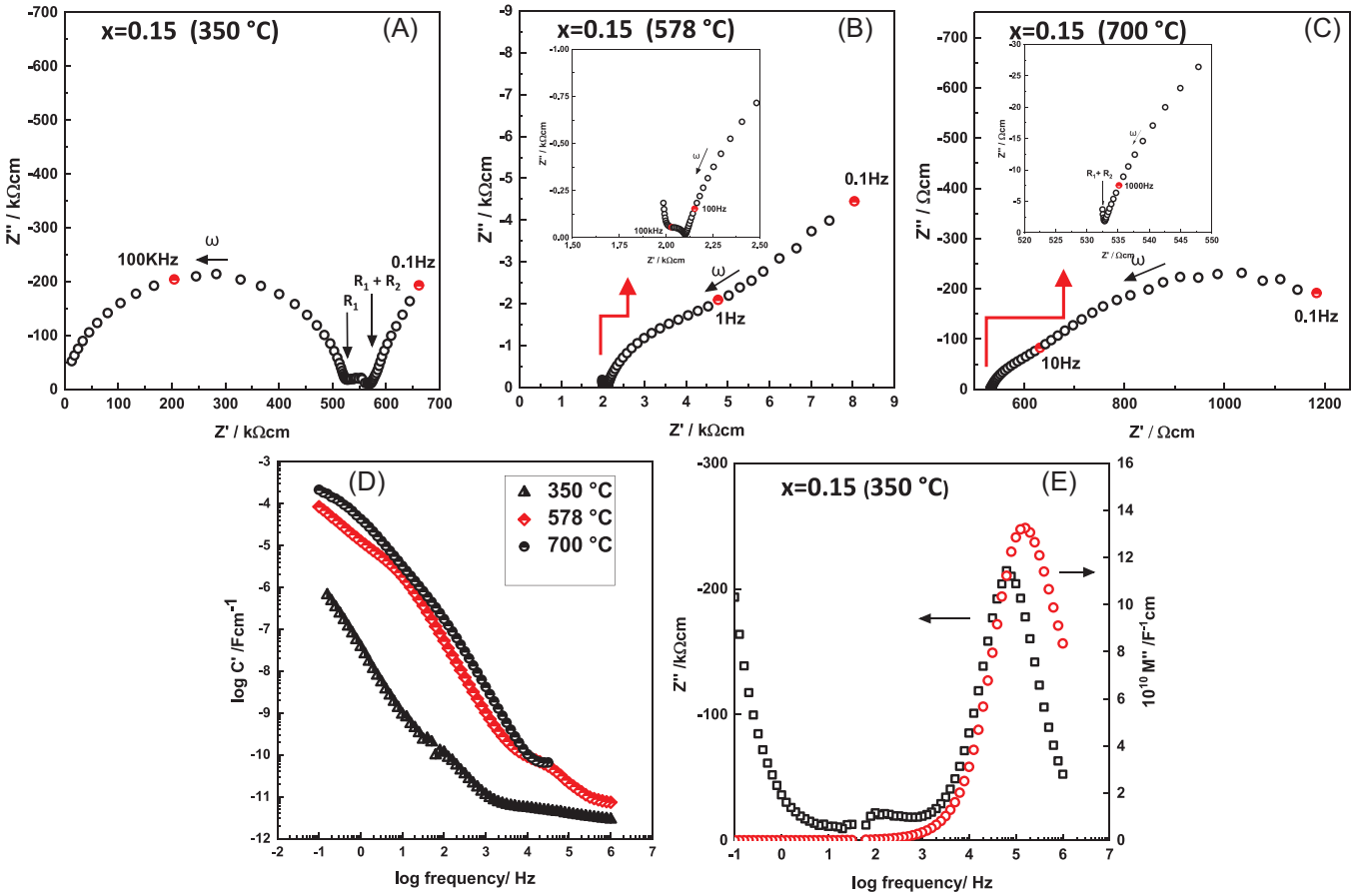

FIGURE 1 For YSH15, impedance complex plane plots, Z* at (A) 350°C, (B) 578°C, and (C) 700°C. (D) C' spectroscopic plots at different temperatures. (E) Z''/ M'' spectroscopic plots.

temperatures. Oxygen partial pressure, pO_2 in the atmosphere is a critical variable in the parameters that control the transition.

A further indication of the effect of pO_2 is shown from the time dependence of resistance data with a voltage close to, but initially below, the OFF-ON switching voltage, in the same three atmospheres and at two temperatures, 501 and 531°C, Figure 3. At 501°C, a small conductivity increase occurs in O_2 but then remains constant in the OFF state. In air and N_2, however, the sample switches to the ON state but slowly, over a period of 5–10 min; the highest ON state conductivity is obtained in N_2. At a somewhat higher temperature, 531°C, the sample switches rapidly to the ON state in all three atmospheres but additional time was required to achieve a steady ON state, especially in N_2.

The time dependence is also seen in removing the dc bias; in air and O_2, the resistance increases to its ground state very rapidly but a few minutes are required to achieve this in N_2. There is some scatter and variation in the final state conductivities with the bias removed which may be caused by the time taken for the sample temperature to adjust to a lower value on effective removal of the Joule heating. These various time-dependent and atmosphere-dependent results indicate further that sample-oxygen exchange, in both directions, is a major factor in controlling voltage-dependent conductivity.

The identity of the charge carriers was determined by a combination of IS measurements in atmospheres of different pO_2 and with a different dc bias applied. A key representative result is shown in Figure 4, with interpretation based on the assumption that the effect of increasing pO_2 was either to create holes by absorption, dissociation, and ionization of oxygen according to, ideally:

$$1/2O_2 \rightarrow O^{2-} + 2h^+ \quad (1)$$

or to trap electrons by:

$$1/2O_2 + 2e^- \rightarrow O^{2-} \quad (2)$$

The distinction between extrinsic *p* and *n* carriers was determined, depending on whether the resistance decreased or increased with changing pO_2. From Figure 4A, the resistance decreases in O_2 at 500°C with a field of 39 V/cm, indicating an increase in *p*-type behavior. This means that under these conditions, the

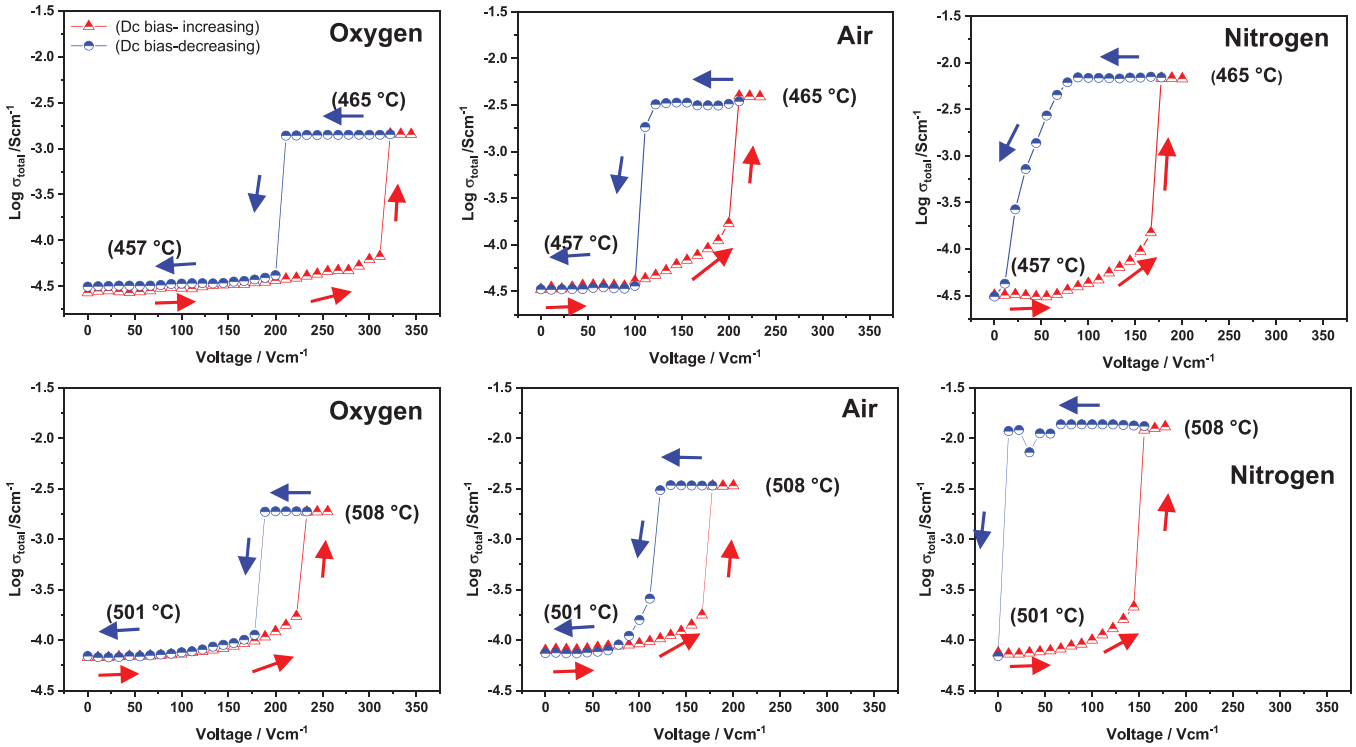

FIGURE 2 Total conductivity of YSH15 after reaching a steady state against applied voltage at 457 and 501°C in atmospheres of different pO_2.

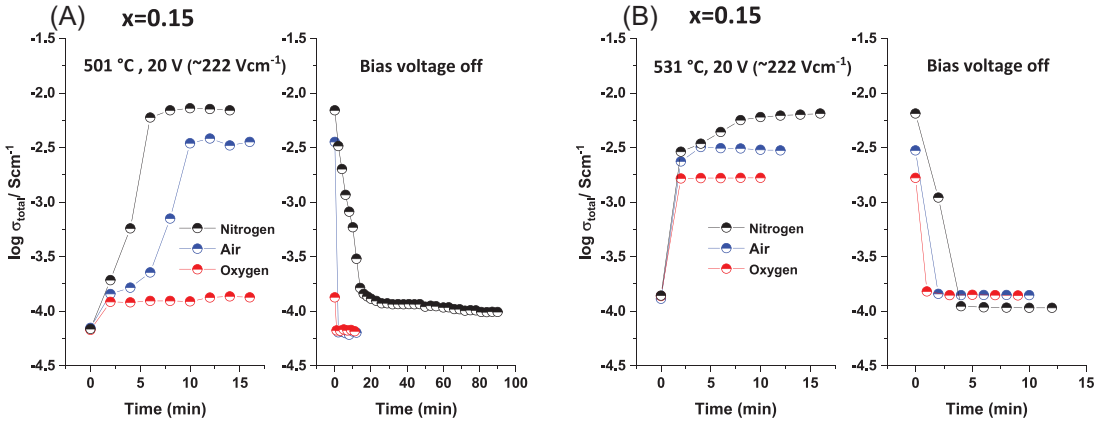

FIGURE 3 Total conductivity of YSH15 versus time on applying and after removing a voltage (A) at 501°C and (B) at 531°C.

majority of charge carriers are holes (p-type) and their conductivity is in parallel with the pre-existing oxide ion conduction.

In order to account for p-type hopping conductivity in materials such as YSH15, it is necessary to determine the location of the holes and, given the absence of cations that can be ionized to a higher oxidation state, the inevitable conclusion is that holes are located on singly-ionized oxygen, as O^- ions. The presence of field-induced p-type conductivity has been observed previously in yttria-doped zirconia ceramics[23–25] similar to the present YSH material and in acceptor-doped $BaTiO_3$ ceramics such as $BaTi_{1-x}Mg_xO_{3-x}$,[26] both of which have oxygen vacancy creation as the main charge compensation mechanism on substitution of the lower valence cations, Y^{3+} for Zr^{4+} and Mg^{2+} for Ti^{4+}, respectively. The p-type conductivity was attributed to the creation of holes on oxide ions by the idealized reaction:

$$O^{2-} \rightarrow O^- + e^- \quad (3)$$

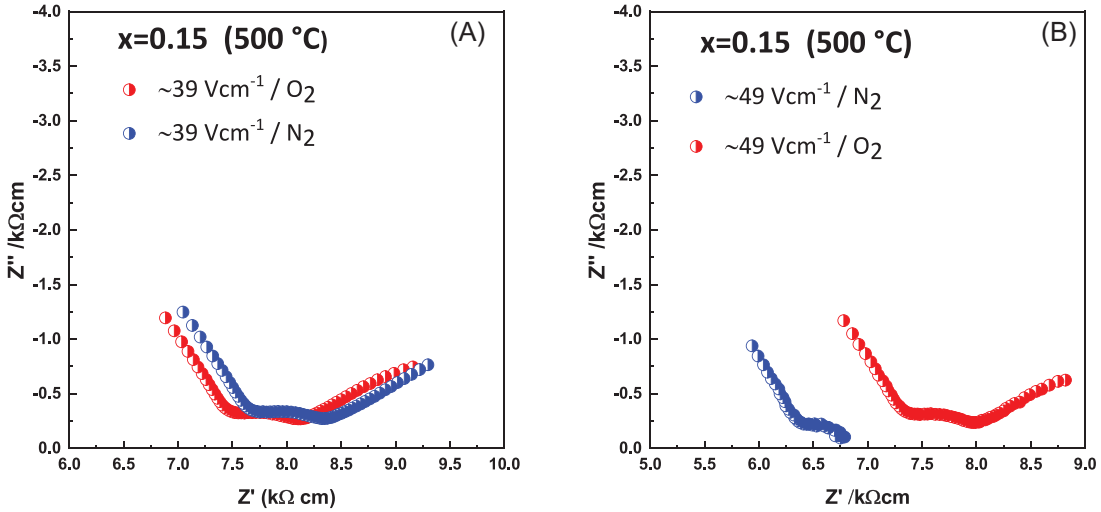

FIGURE 4 Impedance complex plane plots for YSH15 ceramics measured in dry O_2 and N_2 during application of (A) 39 V/cm and (B) 49 V/cm at 500°C. At each voltage, measurements were taken first in dry O_2, and then the atmosphere was changed to dry N_2.

This ionization is associated with under-bonded oxide ions in the vicinity of the acceptor (lower valence) dopant cations; under-bonded oxide ions have a reduced ionization potential, may ionize readily, and are able to undergo spontaneous redox reaction with O_2 molecules from the atmosphere. This leads to O^- ions that occupy the lattice vacancies, V_O, and are the source of resulting *p*-type conductivity:

$$O^{2-} + V_O + 1/2O_2 \leftrightarrow 2O^- \quad (4)$$

Formation of O^- ions by reaction (4) may occur spontaneously, causing materials to be p-type. It can also be promoted in the presence of an applied field, in which case, the liberated electrons, reaction (3), are trapped at the positive electrode. The holes created on oxygen then become the main electronic current carrier and are located initially near the ceramic/positive electrode interface.

On increasing the bias to 49 V/cm, Figure 4B, there was a small decrease in the total resistance in O_2 from ~ 8.2 to 8.0 kΩ cm as more holes were created, but a much greater decrease to ~ 6.75 kΩ cm occurred on switching the atmosphere to N_2. This indicated that at a higher field, the majority of the carriers were n-type and occurred because the sample started to lose oxygen, which liberated more electrons and these became the main charge carrier:

$$O^{2-} \leftrightarrow 1/2O_2 + 2e^- \quad (5)$$

The presence of *n*-type conductivity is widely observed in materials that lose a small amount of oxygen at high temperatures. It appears that a similar reaction to (5) occurs at higher bias fields, which leads to charge injection at the negative electrode. Different reactions occur at the two sample-electrode interfaces, therefore: at the positive electrode, holes are created, reaction (3); at the negative electrode, electrons produced by reaction (5), are injected into the sample.

A detailed study of the temperature and voltage ranges over which p- and n-type behavior dominate the total conductivity has not been made. However, it appears that: first, both types are likely to be present to various degrees under a particular set of conditions; second, p-type behavior, which is associated with single-step ionization of oxide ions, is likely to dominate at lower voltages than those needed for double ionization of oxide ions; third, both ionisations become easier with increasing temperature, as shown by the appearance of n-type behavior at lower voltages with increasing temperature.

Equation (3) represents the first step in the ionization of O^{2-} ions. Oxygen in oxides is traditionally assigned the oxidation state -2 and two-electron transfer is involved in sample-atmosphere interactions that involve an exchange between O^{2-} ions in solid and O_2 molecules in the gas phase; here, it is clear that two steps are involved in oxide ionization. The first leads to O^- ions that remain within the crystal lattice; the second leads to neutral oxygen atoms that are released as molecular O_2. Usually, the two steps are considered to occur simultaneously unless there is a need, as in the present case, for the first step to explain the observation and mechanism of hole creation.

The resistive switching in YSH15 is clearly electronic in origin. The creation of n-type conductivity in ceramics is very well-known, especially associated with oxygen loss at high temperatures. An additional mechanism is required to explain the low field *p*-type conductivity observed

here; several examples of voltage-induced p-type behavior are known in acceptor-doped perovskite- and fluorite-structured ceramics,[21,27–31] similar to that observed with YSH15. Under the action of an applied voltage, *n*-and *p*-type conductivities are initiated at opposite electrodes and, in order to account for the resistive switching, an n-i-p junction is thereby created that has an i region in the ceramic interior. The thicknesses of the *n* and *p* regions are diffusion-controlled, time-dependent, and influenced by surface oxygen exchange interactions with the surrounding atmosphere.

The effect of increasing applied bias, especially in atmospheres of low pO_2, is to increase the amount of oxygen loss, inject more electrons at the negative electrode, increase the thickness of the n-type region, and initiate the breakdown of the n-i-p junction; the breakdown is reversible on removing the source of electrons in the n-type region, leading to the recovery of the original resistance. The recovery does not require the application of a bias voltage and is not, therefore, unipolar or bipolar[1,5] in nature. Instead, the ON-OFF switching appears to involve a threshold switching process which may be a different mechanism to that involved in thin film memristive switching.[1] The breakdown that occurs with increasing dc bias leads to a non-equilibrium state thermodynamically and on the removal of the bias, reaction (5) in particular, is displaced to the left-hand side, leading to the recovery of the p-i-n structure.

4 | CONCLUSIONS

YSH15 is the second example, of which we are aware, of low-field resistive switching in a bulk ceramic. YSH15 shows a reversible increase in conductivity, by 1–3 orders of magnitude, on the application of a small dc voltage. Oxygen partial pressure, pO_2, plays a major role in the resistive-switching behavior. A mechanism for RS is presented based on the effect of dc bias on the conductivity of YSH ceramics. At low voltage, the increase in conductivity is attributed to the introduction of p-type behavior at the positive electrode. The p-type behavior arises from the single ionization of under-bonded O^{2-} ions leading to the creation of holes, located on oxygen as O^{-} ions. At higher voltage, n-type behavior is attributed to oxygen loss by double ionization of oxide ions and injection of electrons at the negative electrode, facilitated by field-induced migration of oxide ions towards the positive electrode. p- and n-type regions are therefore created at opposite electrodes which leads to the creation of a p-i-n structure that, on breakdown, gives an enhancement in the conductivity that is reversible on removal of the bias.

The magnitudes of the applied voltages are above those expected for the typical decomposition potential of ceramic oxides and therefore, YSH15 ceramics in the ON state are kinetically stable but thermodynamically metastable. In addition, the bias fields are several orders of magnitude less than those involved in the operation of nanometer-thick memristors and the detailed switching mechanisms in bulk ceramics are likely to be different.

Voltage-dependent phenomena are fundamental features of two current hot topics in materials science, memristive switching in thin films and flash sintering of bulk ceramics. The discovery of low-field resistive switching in bulk YSH15 ceramics may represent an important link between these two phenomena.

ACKNOWLEDGMENTS

Meshari Alotaibi thanks Taif University for a studentship.

ORCID

Meshari Alotaibi https://orcid.org/0000-0003-1322-6992
Anthony R West https://orcid.org/0000-0002-5492-2102

REFERENCES

1. Lee JS, Lee S, Noh TW. Resistive switching phenomena: a review of statistical physics approaches. Appl Phys Rev. 2015;2(3):031303.
2. Sun W, Gao B, Chi M, Xia Q, Yang JJ, Qian H, et al. Understanding memristive switching via in situ characterization and device modeling. Nat Commun. 2019;10(1):1–13.
3. Wang Z, Wu H, Burr GW, Hwang CS, Wang KL, Xia Q, et al. Resistive switching materials for information processing. Nat Rev Mater. 2020;5(3):173–95.
4. Jeong DS, Thomas R, Katiyar R, Scott J, Kohlstedt H, Petraru A, et al. Emerging memories: resistive switching mechanisms and current status. Rep Prog Phys. 2012;75(7):076502.
5. Sawa A. Resistive switching in transition metal oxides. Mater Today. 2008;11(6):28–36.
6. Yun C, Webb M, Li W, Wu R, Xiao M, Hellenbrand M, et al. High performance, electroforming-free, thin film memristors using ionic $Na_{0.5}Bi_{0.5}TiO_3$. J Mater Chem C. 2021;9(13):4522–31.
7. Walz F. The Verwey transition-a topical review. J Phys Condens Matter. 2002;14(12):R285.
8. García J, Subías G. The Verwey transition—a new perspective. J Phys Condens Matter. 2004;16(7):R145.
9. Waser R, Dittmann R, Staikov G, Szot K. Redox-based resistive switching memories–nanoionic mechanisms, prospects, and challenges. Adv Mater. 2009;21(25-26):2632–63.
10. Cologna M, Prette ALG, Raj R. Flash-sintering of cubic yttria-stabilized zirconia at 750°C for possible use in SOFC manufacturing. J Am Ceram Soc. 2011;94(2):316–9.
11. Raj R, Cologna M, Francis JSC. Influence of externally imposed and internally generated electrical fields on grain growth, diffusional creep, sintering and related phenomena in ceramics. J Am Ceram Soc. 2011;94(7):1941–65.
12. M'Peko J-C, Francis JSC, Raj R. Impedance spectroscopy and dielectric properties of flash versus conventionally sintered

Yttria-Doped Zirconia electroceramics viewed at the microstructural level. J Am Ceram Soc. 2013;96(12):3760–7.
13. Yu M, Grasso S, Mckinnon R, Saunders T, Reece MJ. Review of flash sintering: materials, mechanisms and modelling. Adv Appl Ceram. 2017;116(1):24–60.
14. Mishra TP, Neto RRI, Speranza G, Quaranta A, Sglavo VM, Raj R, et al. Electronic conductivity in gadolinium doped ceria under direct current as a trigger for flash sintering. Scr Mater. 2020;179:55-60.
15. Banerjee W, Kashir A, Kamba S. Hafnium oxide (HfO_2) – a multifunctional oxide: a review on prospect and challenges of hafnium oxide in resistive switching and ferroelectric memories. Small. 2022;18.
16. Schroeder U, Hwang CS, Funakubo H. Ferroelectricity in doped hafnium oxide: materials, properties and devices. Sawston, UK: Woodhead Publishing; 2019.
17. Waser R, Aono M. Nanoionics-based resistive switching memories. Nat Mater. 2007 2007/11/01;6(11):833–40.
18. Kim KM, Jeong DS, Hwang CS. Nanofilamentary resistive switching in binary oxide system; a review on the present status and outlook. Nanotechnology. 2011;22(25):254002.
19. Jung YC, Seong S, Lee T, Kim SY, Park I-S, Ahn J. Improved resistive switching characteristics of a Pt/HfO_2/Pt resistor by controlling anode interface with forming and switching polarity. Appl Surf Sci. 2018;435:117–21.
20. Lin K-L, Hou T-H, Shieh J, Lin J-H, Chou C-T, Lee Y-J. Electrode dependence of filament formation in HfO_2 resistive-switching memory. J Appl Phys. 2011;109(8):084104.
21. Masó N, Beltrán H, Prades M, Cordoncillo E, West AR. Field-enhanced bulk conductivity and resistive-switching in Ca-doped $BiFeO_3$ ceramics. Phys Chem Chem Phys. 2014;16(36):19408–16.
22. Alotaibi M, Li L, West AR. Electrical properties of yttria-stabilized hafnia ceramics. Phys Chem Chem Phys. 2021;23(45):25951–60.
23. Jovaní M, Beltrán-Mir H, Cordoncillo E, West AR. Field-induced pn transition in yttria-stabilized zirconia. Sci Rep. 2019;9; 18538.
24. Masó N, West AR. Electronic conductivity in yttria-stabilized zirconia under a small dc bias. Chem Mater. 2015;27(5):1552–8.
25. Vendrell X, West AR. Induced p-type semiconductivity in yttria-stabilized zirconia. J Am Ceram Soc. 2019;102(10):6100–6.
26. Prades M, Masó N, Beltrán H, Cordoncillo E, West AR. Field enhanced bulk conductivity of $BaTiO_3$:Mg ceramics. J Mater Chem. 2010;20(25):5335-44.
27. Beltrán H, Prades M, Masó N, Cordoncillo E, West AR. Voltage-dependent low-field Bulk resistivity in $BaTiO_3$:Zn Ceramics. J Am Ceram Soc. 2010;93(2):500–5.
28. Masó N, Prades M, Beltrán H, Cordoncillo E, Sinclair DC, West AR. Field enhanced bulk conductivity of acceptor-doped $BaTi_{1-x}Ca_xO_{3-x}$ ceramics. Appl Phys Lett. 2010;97(6):062907.
29. Zhang Q-L, Masó N, Liu Y, Yang H, West AR. Voltage-dependent low-field resistivity of $CaTiO_3$:Zn ceramics. J Mater Chem. 2011;21(34):12894–900.
30. Beltrán H, Prades M, Masó N, Cordoncillo E, West AR. Enhanced conductivity and nonlinear voltage-current characteristics of nonstoichiometric $BaTiO_3$ ceramics. J Am Ceram Soc. 2011;94(9):2951-62.
31. Gil Escrig L, Prades M, Beltrán H, Cordoncillo E, Masó N, West AR. Voltage-Dependent Bulk Resistivity of $SrTiO_3$:Mg Ceramics. J Am Ceram Soc. 2014;97(9):2815–24.

How to cite this article: Alotaibi M, Almutairi F, West AR. Resistive-switching in yttria-stabilized hafnia ceramics. J Am Ceram Soc. 2022;1–7. https://doi.org/10.1111/jace.18821